



UNIVERSITÀ
DEGLI STUDI
FIRENZE

FLORE

Repository istituzionale dell'Università degli Studi di Firenze

UKF-Based Navigation System for AUVs: Online Experimental Validation

Questa è la Versione finale referata (Post print/Accepted manuscript) della seguente pubblicazione:

Original Citation:

UKF-Based Navigation System for AUVs: Online Experimental Validation / Costanzi, Riccardo; Fanelli, Francesco; Meli, Enrico; Ridolfi, Alessandro; Caiti, Andrea; Allotta, Benedetto. - In: IEEE JOURNAL OF OCEANIC ENGINEERING. - ISSN 0364-9059. - STAMPA. - 44:(2019), pp. 633-641. [10.1109/JOE.2018.2843654]

Availability:

This version is available at: 2158/1140675 since: 2021-03-30T15:24:02Z

Published version:

DOI: 10.1109/JOE.2018.2843654

Terms of use:

Open Access

La pubblicazione è resa disponibile sotto le norme e i termini della licenza di deposito, secondo quanto stabilito dalla Policy per l'accesso aperto dell'Università degli Studi di Firenze (<https://www.sba.unifi.it/upload/policy-oa-2016-1.pdf>)

Publisher copyright claim:

Conformità alle politiche dell'editore / Compliance to publisher's policies

Questa versione della pubblicazione è conforme a quanto richiesto dalle politiche dell'editore in materia di copyright.

This version of the publication conforms to the publisher's copyright policies.

(Article begins on next page)

UKF-based Navigation System for AUVs: Online Experimental Validation

Riccardo Costanzi**

Francesco Fanelli*

Enrico Meli*

Alessandro Ridolfi* (*IEEE Member*)

Andrea Caiti** (*IEEE Fellow*)

Benedetto Allotta* (*IEEE Member*)

*Department of Industrial Engineering, University of Florence (UNIFI), Florence, Italy
ISME - Interuniversity Center of Integrated Systems
for the Marine Environment

**Dipartimento di Ingegneria dell'Informazione and Centro di Ricerca "E. Piaggio" -
Università di Pisa (UNIPI), Pisa, Italy
ISME - Interuniversity Center of Integrated Systems
for the Marine Environment

Email: riccardo.costanzi@unipi.it, Email: a.ridolfi@unifi.it

Abstract

Modern Autonomous Underwater Vehicles (AUVs) are currently involved in complex tasks and scenarios, and require accurate and robust navigation systems to estimate their position. However, since the Global Positioning System (GPS) cannot be exploited underwater, the AUV position is not directly measurable in real-time (unless using dedicated acoustic-based sensors), making the availability of a reliable navigation system even more crucial. In this context, the main role is played by the filter used to estimate the AUV motion, usually relying on simple kinematic vehicle models and equations linearization.

A navigation strategy specifically thought for AUVs and based on the Unscented Kalman Filter (UKF) is proposed and experimentally validated by the authors. Preliminary tests of the developed strategy have been carried out by running the navigation filter on experimental data acquired during the FP7 European ARROWS project. This initial validation has been performed totally offline. The AUVs navigated in dead-reckoning without using navigation filters whereas the proposed strategy has been compared to standard Extended Kalman Filter (EKF)-based ones, highlighting encouraging performances.

To further validate the proposed navigation system, suitable sea tests have been performed. The navigation filter has been implemented online on an AUV and the vehicle controller relied only on it to navigate. The new validation procedure, whose results are reported in this paper, showed again the good performance of the chosen strategy, yielding satisfying results in terms of accuracy of vehicle position estimation.

I. INTRODUCTION

Currently, Autonomous Underwater Vehicles (AUVs) are broadly employed in several industrial applications (especially in the Oil&Gas industry), scientific tasks (archaeological exploration and surveillance), military reconnaissance and patrolling missions, search and rescue duties, etc.

An accurate, efficient and robust navigation system, including the suitable hardware and software needed to get a real-time estimation of the vehicle pose, is mandatory for all these kinds of applications [1], [2], [3], [4]. Due to the strict requirements of the modern AUV tasks, involving both single and multiple vehicles [5], [6], [7], [8], [9], precise motion estimation represents the key point in AUV navigation, along with a good trade-off between accuracy and numerical efficiency. Good performance of the navigation system is crucial not only for the results of the mission (e.g. position and attitude errors between desired and real paths, etc.) but also to georeference the experimental data coming from onboard acoustic or optical payload. Furthermore, the Global Positioning System (GPS) information cannot be exploited underwater, complicating both the vehicle localization and the motion estimation, and increasing the importance of an accurate and robust navigation system.

Nowadays, the Kalman Filter (KF) [10] and the Extended Kalman Filter (EKF) (nonlinear KF version) [11], [12], [13] are the main filters exploited for AUV motion estimation. To reach a satisfying trade-off between accuracy, efficiency and memory consumption and to be effectively used in real-time applications, this kind of filters is usually based on simplified kinematic models of the AUV.

An alternative to the EKF is a filtering approach based on the Unscented Kalman Filter (UKF), [14], [15]. Being it computationally affordable by today's AUV hardware and, most of all, derivative free (characteristic that allows it to cope with the difficulties arising using, e.g., the EKF on nonlinear, stiff and non-differentiable systems such as AUVs), it theoretically represents a valid alternative to the most commonly used filters. In recent literature several contributions regarding the use of the UKF in the marine fields can be found. In [16], for example, the authors simulate the behavior of two different real world AUVs during the execution of an autonomous underwater task. Both vehicles are dynamically modeled, and their control loops close on an UKF navigation filter exploiting inertial, velocity and (acoustic) position measurements. The presented results suggest that the UKF may constitute a reliable strategy to estimate the state of a vehicle in the underwater field. In [17], instead, an UKF is used to estimate the kinematic state of an AUV in case of unreliability of sensor measurements. The structure of the filter is suitably modified in order to be able to react to faulty sensor readings, and simulations show the increased robustness of the proposed approach.

64 In addition, in [18], a comparison between the EKF and the UKF is proposed: both filters are used to
65 estimate online the state of a kinematic and dynamic model of an AUV. The state of the system is then
66 augmented to include the unknown hydrodynamic coefficients of the vehicle. Simulation results show that
67 the UKF performs better in estimating both the kinematic state of the vehicle and the unknown coefficients,
68 highlighting the problems faced by the EKF in case of highly nonlinear systems.

69 Despite the encouraging simulation results documented in literature (e.g. the above-mentioned references),
70 to the authors' knowledge, UKF-based approaches have not yet been extensively exploited in practical
71 applications in the underwater field. This led the authors to propose an UKF-based navigation filter specif-
72 ically developed for AUVs. The algorithm relies on the information coming from sensors usually available
73 onboard AUVs (as for instance linear velocity, and depth sensors [19], [20]) and on a mixed kinematic
74 and dynamic AUV model suitably developed and validated, able to provide accurate results if used in
75 conjunction with estimation filters, but not too heavy from a computational viewpoint [21], [22].

76 In previous works, preliminary tests of the UKF-based approach have been carried out by the authors by
77 running the navigation filter on experimental data acquired during the FP7 European ARROWS project [23],
78 [24]. This initial validation has been performed completely offline: sensor data have been used to perform
79 a comparison between an EKF-based navigation filter and the proposed UKF-based one, highlighting the
80 better performance of the latter, especially under critical operating conditions (for instance, with a reduced
81 set of available sensors) [21], [22]. For the sake of clarity, the authors published, till now, intermediate
82 research steps that have been fundamental to reach the actual use in real time of the UKF strategy, which
83 is the achieved final research step described and reported in the present paper. The manuscript is thus not
84 intended to provide a performance comparison with algorithms proposed in the works previously published
85 by the same authors. The navigation strategy here presented is the updated one with a reduced state vector:
86 this is the scheme implemented on board the AUV. The paper is intended as an experimental validation of
87 a navigation system that exploits, as fundamental constituent elements, the most important results achieved
88 and demonstrated in the previous works.

89 After the encouraging results obtained during the first phase of offline validation, subsequent sea tests have
90 been executed in order to validate the proposed approach in a realistic scenario. Different sea test campaigns
91 have been carried out in order to evaluate the performance of the UKF-based navigation filter online: the
92 controller of the vehicle relied only on the filter to navigate. In particular, the results obtained during two
93 sea test campaigns are reported in this paper.

94 After a description of a state-space model of the vehicle given in the following Section, the results obtained
95 during the two above-mentioned sea test campaigns, which took place in Sicily, Italy, in June 2015 and in
96 La Spezia, Italy, in November 2015, are presented in the final Section.

97 II. NAVIGATION FILTER

98 In order to exploit a recursive discrete estimation filter, a suitable discrete state-space formulation of a
99 model of the vehicle must be derived in the form:

$$\begin{cases} \mathbf{x}_k = \mathbf{f}_{k-1}(\mathbf{x}_{k-1}, \mathbf{u}_{k-1}) + \mathbf{w}_{k-1} \\ \mathbf{y}_k = \mathbf{h}_k(\mathbf{x}_k) + \mathbf{v}_k \end{cases}, \quad (1)$$

100 in which \mathbf{x}_k is the state vector at the k -th instant, \mathbf{u}_k and \mathbf{y}_k are the system inputs and outputs, and \mathbf{w}_k
101 and \mathbf{v}_k are additive process and measurement noises, respectively. The first equation in (1) is the *system*
102 *evolution equation* while the second one is the *measurement equation*.

103 The starting point is the complete 6 DOFs dynamic vehicle model proposed by [1]. Then, in a previously
104 published work by the authors [22], this model has been suitably simplified, taking into account only
105 longitudinal dynamics, to derive a mixed kinematic and dynamic model; this model would constitute a
106 convenient trade-off between accuracy and computational load. In [22], the state vector was a twelve-
107 dimensional vector including all the kinematic variables of the AUV (pose and velocity, both linear and
108 angular).

109 At the same time, the authors developed an efficient attitude estimation filter [25], which is able to estimate
110 the orientation of the vehicle even in presence of magnetic disturbances, hence removing the need of
111 estimating the attitude and the angular velocity of the AUV within its navigation filter. For this reason,
112 the authors decided to reduce the dimension of the state vector with respect to [22], considering attitude a
113 time-varying input instead of a state component; i.e. in the real scheme implemented on board the AUV,
114 the authors use algorithms dedicated to the estimation of the vehicle orientation and this is the reason why
115 it is possible to use the AUV angles as inputs for the UKF-based position estimation. The UKF position
116 estimation algorithm is a good choice for the non-linear behaviour of the AUV. The used orientation
117 estimator [25] is useful during real missions at sea because it is able to face the quite common magnetic
118 disturbances present in the environment. From the application point of view, the authors thus believe that
119 both algorithms (UKF and attitude estimation algorithm) are important for high performance navigation
120 systems.

121 Taking into account the above-mentioned considerations, and using SNAME notation [1], the resulting state
 122 vector can be properly defined as:

$$\mathbf{x} = \begin{bmatrix} \boldsymbol{\eta}_1 \\ \boldsymbol{\nu}_1 \end{bmatrix}. \quad (2)$$

123 where the state vector \mathbf{x} is composed of Earth-fixed position $\boldsymbol{\eta}_1$ and body-fixed linear velocity $\boldsymbol{\nu}_1$ of the
 124 AUV. The discrete-time system state evolution equation is given by:

$$\begin{bmatrix} \boldsymbol{\eta}_1 \\ \boldsymbol{\nu}_1 \end{bmatrix}_k = \begin{bmatrix} \boldsymbol{\eta}_1 \\ \boldsymbol{\nu}_1 \end{bmatrix}_{k-1} + \begin{bmatrix} R_B^N((\boldsymbol{\eta}_2)_{k-1}) (\boldsymbol{\nu}_1)_{k-1} \\ \frac{\tau_{1x}(\boldsymbol{\nu}_{k-1}, \mathbf{u}_{k-1})}{m} + \frac{F_1(\boldsymbol{\nu}_{k-1})}{m} \\ 0 \\ 0 \end{bmatrix} + \mathbf{w}_{k-1}, \quad (3)$$

125

126 where $R_B^N(\boldsymbol{\eta}_2)$, function of the orientation of the vehicle $\boldsymbol{\eta}_2$, is the rotation matrix from a fixed *North-East-Down* (NED) frame N to the body-fixed frame B , $\tau_{1x}(\boldsymbol{\nu}, \mathbf{u})$ is the force acting on the vehicle longitudinal
 127 axis as a nonlinear function of its velocity and of the rotating speeds of its propellers \mathbf{u} , m is the mass of
 128 the vehicle, ΔT is the fixed filter sampling time, and $F_1(\boldsymbol{\nu})$ is the hydrodynamic damping force acting on
 129 the longitudinal degree of freedom, given by:

$$F_1(\boldsymbol{\nu}_{k-1}) = -\frac{A_f C_u \rho (\nu_{1x})_{k-1}^2 \operatorname{sgn}(\nu_{1x})_{k-1}}{2}, \quad (4)$$

131 being A_f and C_u the “reference frontal area” of the AUV and the longitudinal drag coefficient [26].

132 For a detailed derivation of the terms of (3), including the propulsion system modeling, please refer to [22],
 133 [27].

134 For what concerns the measurement equation, the available physical quantities are the sensors outputs:

$$\mathbf{y}_k = \begin{bmatrix} \eta_{1x}^{GPS} & \eta_{1y}^{GPS} & \eta_{1z}^{DS} & (\boldsymbol{\nu}_1^{DVL})^T \end{bmatrix}_k^T, \quad (5)$$

135 where the GPS (on surface) and the depth sensor (DS) are used to measure $\boldsymbol{\eta}_1$, while the Doppler Velocity
 136 Logger (DVL) is used to measure $\boldsymbol{\nu}_1$. Please refer to table I for the main characteristics of the considered
 137 vehicle, including a sensor list.

138 (5) highlights that the measurement equation is affine. More particularly, the measurement function $\mathbf{h}_k(\cdot)$
139 can be expressed through a matrix H_k containing only 1 or 0 elements:

$$\mathbf{y}_k = H_k \mathbf{x}_k + \mathbf{v}_k . \quad (6)$$

140 The size of the matrix H_k may vary over the time. In fact, the vehicle sensors are characterized by different
141 working frequencies but the filter sample time ΔT is fixed. Consequently, since each sensor is queried for
142 a new measurement at each sampling period, if such measurement is not available, the corresponding rows
143 of H_k must be deleted. In the proposed navigation strategy, the GPS is used for the correction step each
144 time it is available. I.e. GPS data are always used for the correction when the vehicle is on surface, while
145 instead they are not available when the AUV is navigating underwater.

146 Considering Equations (3)-(4), the resulting vehicle model is highly nonlinear and non-differentiable; for
147 this reason, linear filters, such as the standard Kalman Filter [10], cannot be used to estimate the state of
148 the vehicle. Additionally, even strategies based on the Extended Kalman Filter [11], [12], [13] could lead
149 to important accuracy problems. These reasons motivated the authors to investigate alternative estimation
150 strategies. A navigation filter based on the Unscented Kalman Filter [11], [14], [15] has then been chosen,
151 since it is completely derivative free and the hardware which is today present on AUVs is able to efficiently
152 handle the required computational load. However, despite the above-mentioned advantages, the authors could
153 not find in literature extensive sources of its exploitation in practical underwater operations; for instance,
154 taking into account the state of the art of the last years, analyzed in the Introduction, only completely
155 simulated results or offline simulations exploiting experimental sensor data can be found.

156 At first, after developing the vehicle model described in [22], the authors performed an offline comparison
157 between the proposed UKF-based strategy and an EKF-based navigation filter (exploiting real sensor data
158 acquired during experimental missions), highlighting the advantages of the UKF, especially when the sensor
159 set is reduced. The results of such tests can be found in [21], [22]. The positive outcomes of this preliminary
160 comparison encouraged the authors to test the UKF-based strategy online, simplifying the original vehicle
161 model as described at the beginning of this Section and implementing the filter onboard. Then, suitable
162 experimental tests have been carried out in order to evaluate the online performance of the proposed solution
163 in a real scenario. The obtained results at sea are reported in the following Section.

III. EXPERIMENTAL TESTS AND VALIDATION

165 This Section reports the results obtained during two different test campaigns, which took place, respec-
 166 tively, in June 2015 and in November 2015. The UKF-based navigation filter described in the previous
 167 Section has been integrated within the control architecture of the vehicle, which is based on ROS (*Robot*
 168 *Operating System*); the performed tests aimed at validating online the proposed strategy.

169 The used vehicle is the Typhoon AUV, developed and built by the Department of Industrial Engineering of
 170 the University of Florence (DIEF) during the THESAURUS Tuscany Region project [28] and the European
 171 ARROWS project [23] (Figure 1). The main features of the vehicle are given in Table I. Both the missions
 172 presented in the paper, starting from the first waypoints WP1, are performed underwater (the AUV is at a
 173 certain depth); thus, GPS data are not available from WP1 till the end of each mission - final resurfacing
 (no other resurfacings are present) - and cannot be used for the correction step. In the remaining of this

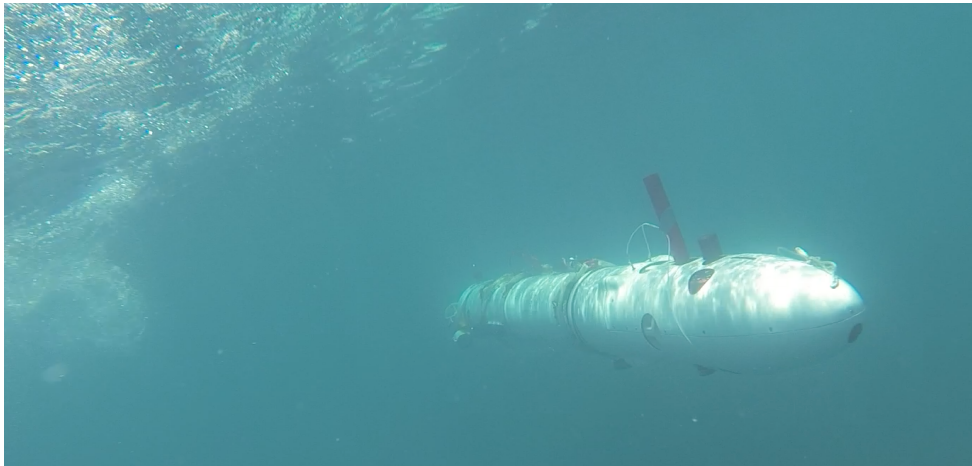


Fig. 1: Typhoon AUV

Typhoon AUV main characteristics	
Size [mm]	3600×350 (diameter) approx.
Mass [kg]	130-180 (dep. on payload)
Max speed [kn]	5-6
Max depth [m]	300
Autonomy [h]	8
Navigation sensors	GPS, IMU, FOG, DVL, depth sensor, acoustic modem
Payload	cameras, 2D forward-looking sonar, side-scan sonar

TABLE I: Typhoon AUV physical data, payload and performance

175 Section, the results obtained during the two test campaigns are analyzed in details.

176 A. Sicily, Italy, June 2015 test campaign

177 This experimental campaign was performed near the *Cala Minnola* wreck (Levanzo, Aegadian Islands,
178 Sicily, Italy) during the first final demonstration of the ARROWS project (May 25 - June 5, 2015, [23], [24]).
179 Typhoon AUV was required to autonomously follow the transept-shaped path shown in Figure 2. The path
180 consisted of 16 waypoints (from WP1 to WP16) and its sizes were about 27 m per 55 m (total length equal
181 to about 464 m); the GPS coordinates of the point WP1 are 37.9891° N and 12.3547° E. The AUV navigated
182 underwater at a depth of about 25 m and at a constant altitude of 2 m from the seabottom whereas the
183 longitudinal speed was controlled at 0.5 m/s. A non-negligible sea current was present during the test day,
approximately directed in North-South direction. An Ultra Short BaseLine (USBL) transducer was mounted

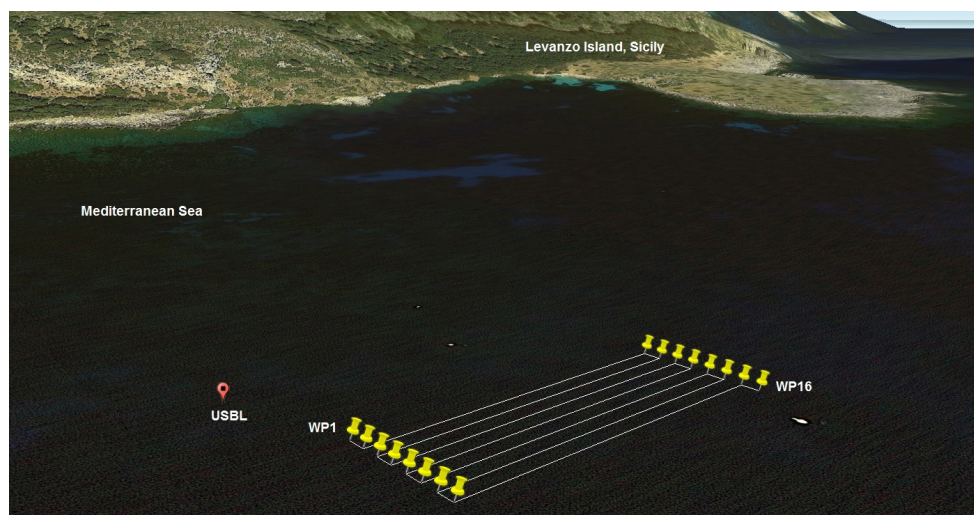


Fig. 2: The transept-shaped path followed by the Typhoon AUV during the sea tests near the *Cala Minnola* wreck (Levanzo, Aegadian Islands, Sicily, Italy)

184

185 on a support ship near the planned path, as shown in Figure 2, and was used for mission monitoring. The
186 measured AUV position, not used as a correction term within the filter, can be considered the ground truth.
187 The position of Typhoon was measured through such sensor and its data were made available to Typhoon
188 through acoustic communication. It is worth noting that thus the USBL orientation was not constant and
189 this may affect the localization measurement accuracy. For the sake of clarity, this measurement system
190 suffers from a certain error due to the combination of: the intrinsic measurement error of the USBL device
191 itself, the measurement error of the GPS and the measurement error of the IMU mounted on the buoy, the
192 possible synchronization error of these onboard (on the buoy) data, [29]. Nevertheless its outputs, given
193 in Figure 5, were consistent with similar results reported in literature (see for example [30]). In Figure 3,
194 the vehicle position estimated by the navigation algorithm $[\eta_{1x}^{UKF} \ \eta_{1y}^{UKF}]^T$ is reported and compared to the

195 ideal vehicle position based on the predefined waypoints $[\eta_{1x}^{ID} \ \eta_{1y}^{ID}]^T$. Although the disturbance due to the
 196 sea current is visible during the first legs of the transept and no current estimators are exploited into the
 197 navigation filter, the results are quite encouraging and highlight the goodness of the proposed approach.
 The good estimation of the vehicle position provided by the navigation algorithm allowed, among the other

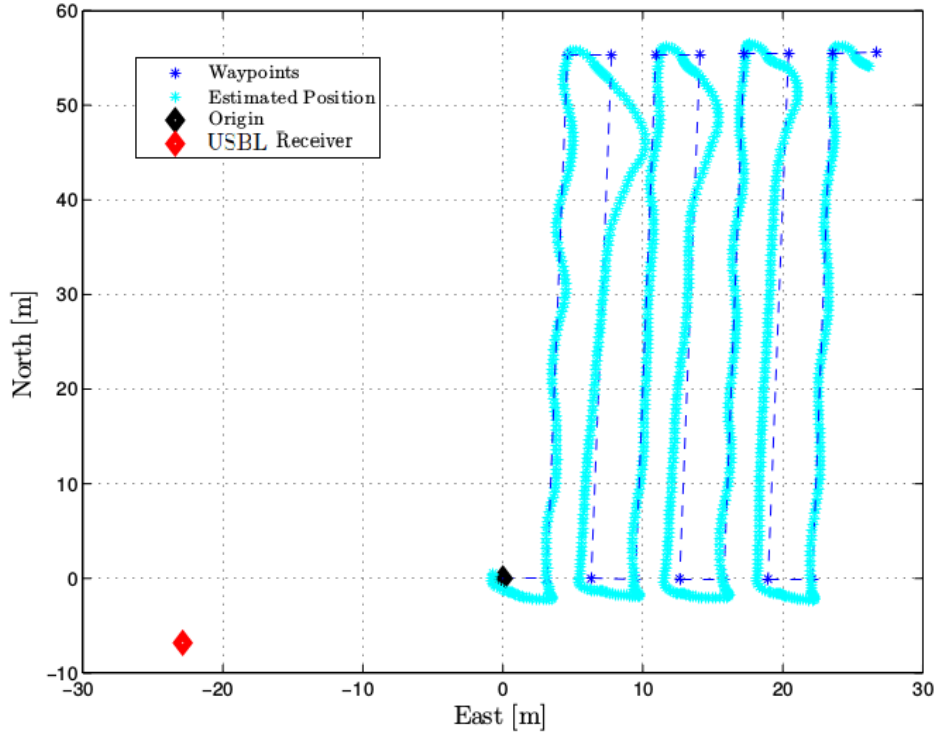


Fig. 3: Comparison between the vehicle position estimated by the navigation algorithm $[\eta_{1x}^{UKF} \ \eta_{1y}^{UKF}]^T$ and the ideal vehicle position based on the predefined waypoints $[\eta_{1x}^{ID} \ \eta_{1y}^{ID}]^T$

198
 199 benefits, the accurate mapping and reconstruction of the archeological site of the *Cala Minnola* wreck ([23],
 200 [24]). As an example, an optical frame captured by the vehicle during the mission is reported in Figure 4.
 201 Some of the obtained 3D reconstructions are available on the ARROWS project website [23].
 202 From a quantitative point of view, the estimation errors $\|\eta_1^{UKF} - \eta_1^{USBL}\|$ between the vehicle position
 203 estimated by the navigation algorithm and the vehicle position provided by the USBL are summarized
 204 in Figure 5, in correspondence of the USBL fixes. The USBL fixes are quite numerous and uniformly
 205 distributed in time, allowing a reliable assessment of the performance of the navigation algorithm. The
 206 error trend here reported is associated with the vehicle navigating underwater; i.e. the origin of the time
 207 line of Figure 5 coincides with the AUV immersion phase. Thus as concerns the time slot of the error
 208 trend, GPS data are not available (the AUV is at depth) and cannot be used for the correction step. Despite



Fig. 4: An optical frame captured during the mapping of the archeological site of the *Cala Minnola* wreck (Levanzo, Aegadian Islands, Sicily, Italy)

209 the uncertainty affecting the USBL measurements, the error caused by the USBL sensor (see for example
210 [30]) and the effect of the sea currents, the global estimation error is limited (less than 5 m), highlighting
211 the good performance of the navigation algorithm.

212 *B. La Spezia, Italy, November 2015 test campaign*

213 The second test campaign presented in this paper was carried out on November 19, 2015 in a sea basin
214 in the harbor of La Spezia, Italy. During the mission, Typhoon autonomously performed the transept-shaped
215 path shown in Figure 6. The ideal trajectory was composed of 8 different waypoints (from WP1 to WP8)
216 and its sizes were about 10 m per 80 m (total length equal to about 350 m); the GPS coordinates of
217 the point WP1 are 44.09468695° N and 9.862218645° E. While executing its task, Typhoon navigated
218 underwater (depth of about 3 m) at a fixed desired longitudinal speed equal to 0.5 m/s. Close to the mission
219 path, a fixed reference buoy (Figure 6) equipped with an USBL transducer, an Inertial Measurement Unit
220 (IMU) and a GPS (to estimate its own pose) was placed on the water surface. The buoy (GPS coordinates
221 44.09506073° N and 9.86148400° E) transmitted the data needed for mission monitoring directly to the
222 shore through a proper a WiFi access point. The USBL sensor allowed to determine the AUV position at

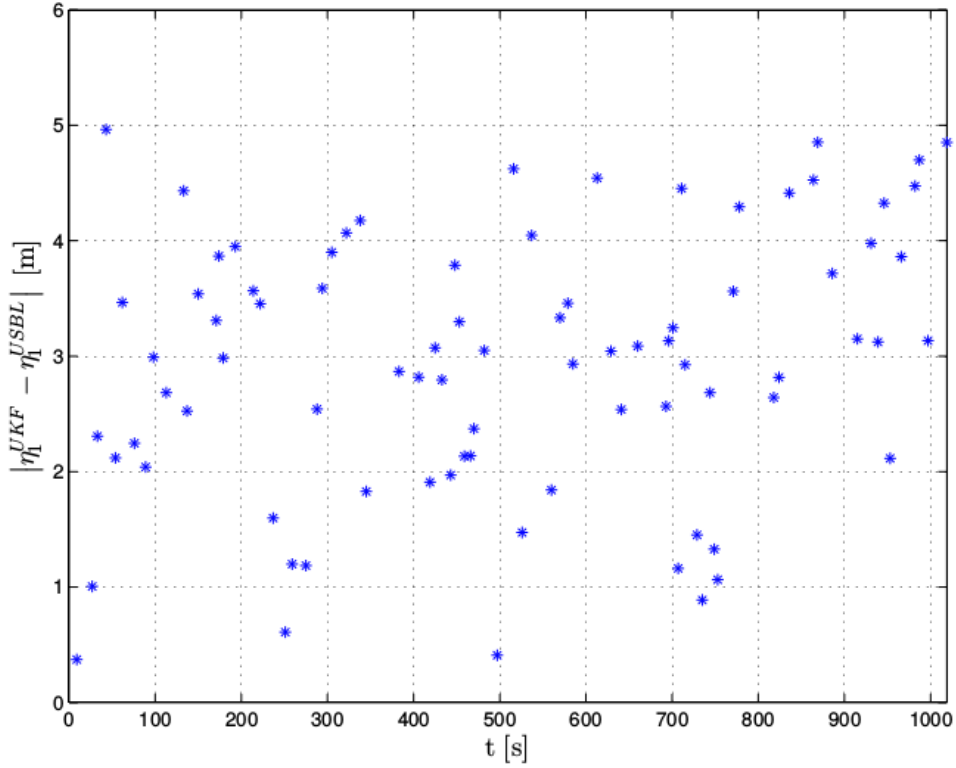


Fig. 5: Estimation errors $\|\eta_1^{UKF} - \eta_1^{USBL}\|$ between the vehicle position estimated by the navigation algorithm and the vehicle position provided by the USBL (in correspondence of the USBL fixes)

223 high rate and sent an acoustic ping after each vehicle localization. Thanks to the USBL, the trajectory of
 224 the AUV was measured according to the accuracy of the sensor. Similarly to the previous test campaign,
 225 such measurement was then exploited as ground truth to investigate the performance of the UKF navigation
 226 algorithm implemented into the AUV motion controller.

227 It is important to point out that the USBL pose was not exactly constant. This may negatively influence the
 228 accuracy of the USBL measurements; however, the quality of the data provided by the USBL during the
 229 experimental campaign (see Figure 9) turned out to be numerically similar to those of other studies present
 230 in literature [30].

231 The AUV position provided by the navigation filter $[\eta_{1x}^{UKF} \ \eta_{1y}^{UKF}]^T$ and the reference AUV trajectory
 232 obtained connecting the desired waypoints $[\eta_{1x}^{ID} \ \eta_{1y}^{ID}]^T$ are compared in Figure 7. A specific zoom of the
 233 estimated and ideal vehicle positions $[\eta_{1x}^{UKF} \ \eta_{1y}^{UKF}]^T$, $[\eta_{1x}^{ID} \ \eta_{1y}^{ID}]^T$ near to the waypoints WP6 and WP7
 234 is highlighted in Figure 8. As for the first test campaign, even if the system is characterized by several
 235 sources of uncertainty (e.g. error on the USBL sensor positioning due to residual motions of the reference
 236 buoy and the intrinsic error of the USBL sensor), the resulting online AUV position estimation error is



Fig. 6: The transept-shaped path followed by the Typhoon AUV during the sea tests in La Spezia, Italy

237 quite limited, confirming the satisfying performance of the proposed navigation filter shown in previous
238 tests.

239 Finally, the authors would like to highlight that in the two missions proposed in the paper (error results
240 given in Figures 5 and 9) it is hard to appreciate the increase in the position error drift, even if present
241 for sure. This is due not only to the adopted ground truth but also because the strategy/system illustrated
242 in the paper exploits a quite performing sensor set, e.g. a DVL and a FOG on board (please refer e.g. to
243 [31] to see that with good sensors the error can be very limited even with just a dead reckoning navigation
244 strategy); the error thus does not grow quickly during time. If the error grows slowly it is not simple to
245 appreciate its drift in the time slots related to the experimental campaigns at sea made here in Italy and
246 reported in the paper. However, the slowly growing error achieved in both the mission is a good point
247 because the AUV is not obliged to perform frequent resurfacings to get the position reset. These results
248 have the aim to validate the UKF navigation strategy, not too much widespread in the underwater robotics
249 field nowadays, and considering this aim they are consistent and satisfying.

250

IV. CONCLUSION

251 In this paper, the authors studied and validated an UKF-based navigation algorithm especially developed
252 for AUVs. The navigation algorithm has been experimentally tested directly online on the Typhoon AUV,
253 developed and built by the University of Florence in the framework of the Tuscany Region THESAURUS

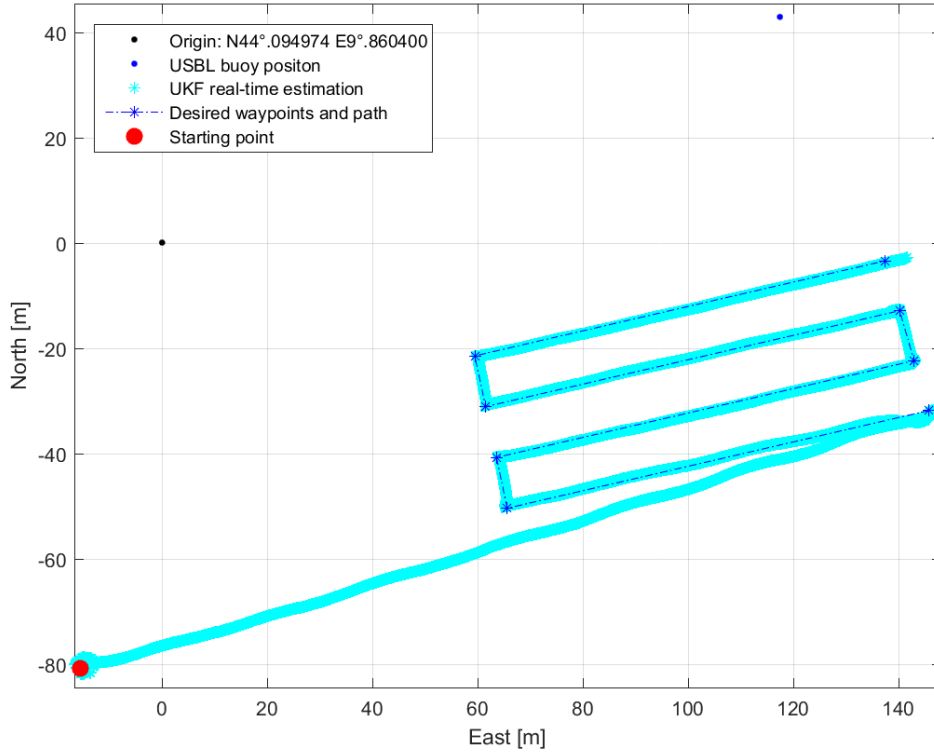


Fig. 7: Comparison between the vehicle position estimated by the navigation algorithm $[\eta_{1x}^{UKF} \ \eta_{1y}^{UKF}]^T$ and the ideal vehicle position based on the predefined waypoints $[\eta_{1x}^{ID} \ \eta_{1y}^{ID}]^T$ (the GPS coordinates of the point WP1 are 44.09468695° N and 9.862218645° E)

254 project [28] and of the FP7 European ARROWS project [23], [24]. Suitable experimental tests have been
 255 carried out to validate online the proposed strategy, and this paper reports the results obtained during two
 256 of these test campaigns.

257 This first online validation of the navigation system yielded satisfying results. The navigation algorithm
 258 showed good accuracy in estimating the vehicle position, even in presence of environmental disturbances
 259 such as sea currents which may deeply influence the navigation system accuracy. The complete navigation
 260 algorithm performs a real-time (the algorithm here proposed is implemented online within the motion
 261 control loop) pose (both position and orientation) estimation that contemporarily exploits the positive results
 262 achieved in previous works by the same authors, and till now validated only singularly and off-line through
 263 post-processing analysis of data logged in various experiments of the past. In addition, it is worth pointing
 264 out that the results presented in this manuscript did not highlight discrepancies with respect to what was
 265 obtained in the previous works; on the contrary, the online experimental validation of the proposed algorithm,
 266 that combines the approaches of position and orientation estimation within a whole strategy (based on the

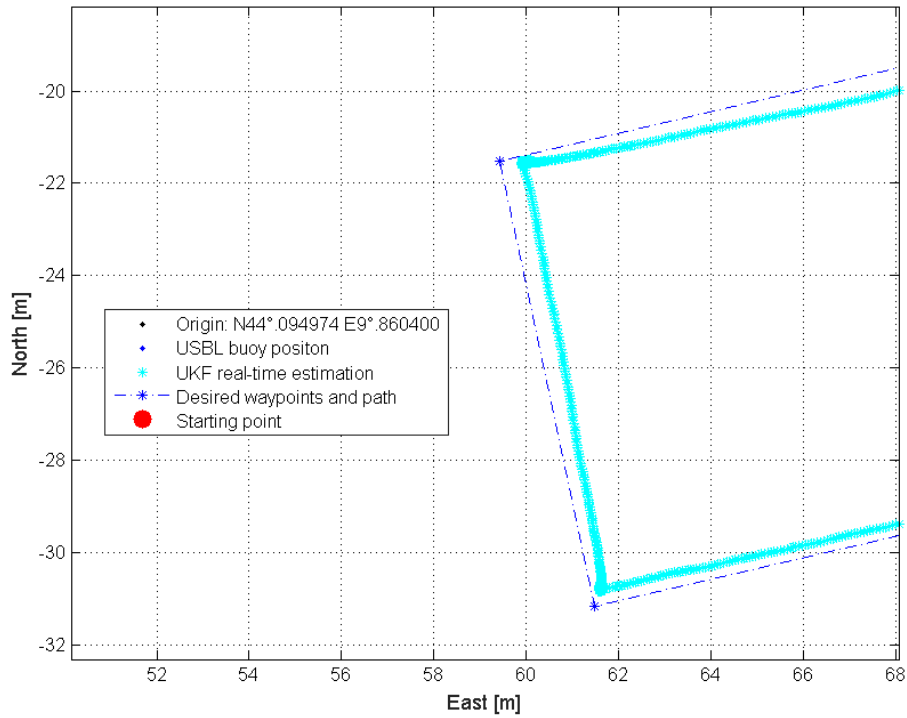


Fig. 8: Zoom of the estimated and ideal vehicle positions $[\eta_{1x}^{UKF} \ \eta_{1y}^{UKF}]^T$, $[\eta_{1x}^{ID} \ \eta_{1y}^{ID}]^T$ near to the waypoints WP6 and WP7

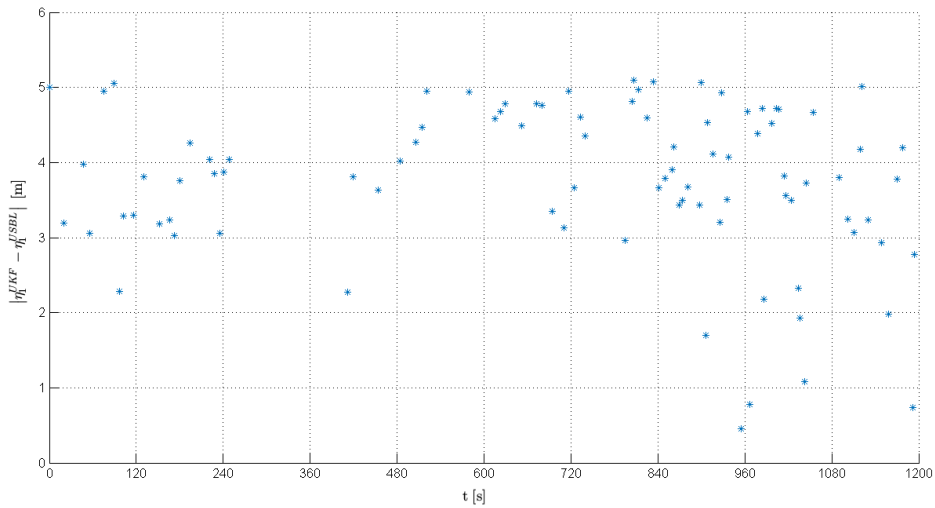


Fig. 9: Estimation errors $\|\eta_1^{UKF} - \eta_1^{USBL}\|$ between the vehicle position estimated by the navigation algorithm and the vehicle position provided by the USBL in correspondence of the USBL fixes

267 described new, modified version of UKF), provided results coherent with them. The navigation algorithm
 268 allowed the vehicle to navigate underwater without problems related to its own pose estimation.
 269 As regards the further developments of this research activity, the UKF-based navigation filter will be

270 validated again on different AUVs belonging to the University of Florence in more complex tasks. This
271 way, the reliability of the proposed navigation strategy will be better investigated. Subsequently, sea current
272 estimators will be studied and implemented on the AUVs and tested online to further improve the filter
273 robustness and to better understand the influence of the sea currents on the AUV dynamics.

274 ACKNOWLEDGMENTS

275 The described work has been partially supported by ARROWS project (it has received funding from
276 the European Union's Seventh Framework Programme for research, technological development and demon-
277 stration under grant agreement no. 308724), BRUCE project (it has received funding from the European
278 Union's Seventh Framework Programme within "SUNRISE - Open Call 2 for new beneficiaries", under
279 grant agreement no. 611449), WiMUST project (it has received funding from the European Union's Horizon
280 2020 research and innovation program under grant agreement no. 645141), THESAURUS project (PAR FAS
281 REGIONE TOSCANA Linea di Azione 1.1.a.3).

282 REFERENCES

- 283 [1] T. Fossen, Ed., *Guidance and Control of Ocean Vehicles*. John Wiley and Sons, London, UK, 1994.
- 284 [2] B. Siciliano and O. Khatib, Eds., *Handbook of Robotics*. Springer Handbooks, Stanford, CA, USA, 2001.
- 285 [3] G. Antonelli, Ed., *Underwater Robots*. Springer-Verlag, Heidelberg, Germany, 2006.
- 286 [4] A. Caffaz, A. Caiti, G. Casalino, and A. Turetta, "The Hybrid Glider/AUV Folaga," *IEEE Robotics and Automation Magazine*, vol. 17,
287 pp. 31–40, 2010.
- 288 [5] A. Vasilijevic, D. Nad, F. Mandic, N. Miskovic, and Z. Vukic, "Coordinated Navigation of Surface and Underwater Marine Robotic
289 Vehicles for Ocean Sampling and Environmental Monitoring," *IEEE/ASME Transactions on Mechatronics*, 2017.
- 290 [6] N. Tsiokgas, Z. Saigol, and D. Lane, "Distributed multi-AUV cooperation methods for underwater archaeology," in *Proceedings of*
291 *MTS/IEEE OCEANS 2006*, 2015.
- 292 [7] M. Breivik and T. I. Fossen, "Guidance-Based Path Following for Autonomous Underwater Vehicles," in *Proceedings of the IEEE*
293 *OCEANS 2005*, Washington D.C., USA, 2005.
- 294 [8] C. Petres, Y. Pailhas, P. Patron, Y. Petillot, J. Evans, and D. Lane, "Path Planning for Autonomous Underwater Vehicles," *IEEE*
295 *Transactions on Robotics*, vol. 23, pp. 331–341, 2007.
- 296 [9] O. Fjellstad and T. I. Fossen, "Position and Attitude Tracking of AUVs: A Quaternion Feedback Approach," *IEEE Journal of Oceanic*
297 *Engineering*, vol. 19, pp. 512–518, 1994.
- 298 [10] R. E. Kalman, "A new approach to linear filtering and prediction problems," *Journal of Basic Engineering*, vol. 82, pp. 35–45, 1960.
- 299 [11] Y. Bar-Shalom, X. R. Li, and T. Kirubarajan, Eds., *Estimation with Applications to Tracking and Navigation*. Wiley and Sons, New
300 York, NY, USA, 2001.
- 301 [12] G. Evensen, Ed., *Data Assimilation*. Springer Verlag, Heidelberg, Germany, 2009.

- 302 [13] A. H. Sayed, Ed., *Adaptive Filters*. Wiley and Sons, Hoboken, NJ, USA, 2009.
- 303 [14] S. Julier and J. Uhlmann, "Unscented Filtering and Nonlinear Estimaion," *Proceedings of the IEEE*, vol. 92, pp. 401–422, 2004.
- 304 [15] E. A. Wan and R. V. D. Merwe, Eds., *The Unscented Kalman Flter*. S. Haykin Edition, New York, NY, USA, 2001.
- 305 [16] M. Barisic, A. Vasilijevic, and D. Nad, "Sigma-Point Unscented Kalman Filter Used For AUV Navigation," in *20th Mediterranean*
306 *Conference on Control & Automation (MED)*, Barcelona, Spain, 2012.
- 307 [17] C. Hajiyev, M. Ata, M. Dinc, and H. Soken, "Fault tolerant estimation of autonomous underwater vehicle dynamics via robust UKF,"
308 in *13th International Carpathian Control Conference*, Barcelona, Spain, 2012.
- 309 [18] M. Sabet, P. Sarhadi, and M. Zarini, "Extended and Unscented Kalman filters for parameter estimation of an autonomous underwater
310 vehicle," *Ocean Engineering*, vol. 91, pp. 329–339, 2014.
- 311 [19] F. Arrichiello, G. Antonelli, A. P. Aguiar, and A. Pascoal, "Observability metric for the relative localization of AUVs based on range
312 and depth measurements: Theory and experiments," in *IEEE/RSJ International Conference on Intelligent Robots and Systems (IROS)*,
313 San Francisco, CA, USA, 2011.
- 314 [20] P. Rigby, O. Pizarro, and S. Williams, "Towards Geo-Referenced AUV Navigation Through Fusion of USBL and DVL Measurements,"
315 in *Proceedings of MTS/IEEE OCEANS 2006*, Boston, MA, USA, 2006.
- 316 [21] B. Allotta, A. Caiti, L. Chisci, R. Costanzi, F. D. Corato, F. Fanelli, C. Fantacci, D. Fenucci, E. Meli, and A. Ridolfi, "Comparison
317 between EKF-based and UKF-based navigation algorithms for AUVs localization," in *Proceedings of the IEEE OCEANS 2015*, Genova,
318 Italy, 2015.
- 319 [22] B. Allotta, A. Caiti, R. Costanzi, F. Fanelli, D. Fenucci, E. Meli, and A. Ridolfi, "A new AUV navigation system exploiting unscented
320 Kalman filter," *Ocean Engineering*, vol. 113, pp. 121–132, 2016.
- 321 [23] ARROWS Project, "<http://www.arrowsproject.eu>," *Official Site of the European ARROWS Project*, 2015.
- 322 [24] B. Allotta, R. Costanzi, and A. Ridolfi, "The ARROWS project: adapting and developing robotics technologies for underwater
323 archaeology," in *Proceedings of IFAC Workshop on Navigation Guidance and Control of Underwater Vehicles (NGCUV 2015)*, Girona,
324 Spain, 2015.
- 325 [25] R. Costanzi, F. Fanelli, N. Monni, A. Ridolfi, and B. Allotta, "An Attitude Estimation Algorithm for Mobile Robots Under Unknown
326 Magnetic Disturbances," *IEEE/ASME Transactions on Mechatronics*, vol. 21, pp. 1900–1911, August 2016.
- 327 [26] B. Munson, A. Rothmayer, T. Okiishi, and W. Huebsch, Eds., *Fundamentals of Fluid Mechanics*. John Wiley and Sons, 2012.
- 328 [27] B. Allotta, A. Caiti, L. Chisci, R. Costanzi, F. D. Corato, C. Fantacci, D. Fenucci, E. Meli, and A. Ridolfi, "An unscented Kalman filter
329 based navigation algorithm for autonomous underwater vehicles," *Mechatronics*, vol. 39, pp. 185–195, 2016.
- 330 [28] THESAURUS Project, "<http://thesaurus.isti.cnr.it>," *Official Site of the Italian THESAURUS Project*, 2013.
- 331 [29] R. Costanzi, N. Monni, A. Ridolfi, B. Allotta, and A. Caiti, "On field experience on underwater acoustic localization through USBL
332 modems," in *Proceedings OCEANS 2017 MTS/IEEE Aberdeen*, Aberdeen, Scotland, 2017.
- 333 [30] L. Christensen, M. Fritsche, J. Albiez, and F. Kirchner, "USBL pose estimation using multiple responders," in *Proceedings MTS/IEEE*
334 *Conference and Exhibition OCEANS 2010*, Sidney, Australia, 2010.
- 335 [31] Ø. Hegrens, A. Ramstady, T. Pedersen, and D. Velasco, "Validation of a new generation DVL for underwater vehicle navigation," in
336 *Proceedings 2016 IEEE/OES Autonomous Underwater Vehicles (AUV)*, Tokyo, Japan, 2016.